# Nucleation of lamellar domains from a sponge phase under shear flow: Shape selection of nuclei in a nonequilibrium steady state

Hideyuki Miyazawa* and Hajime Tanaka†
*Institute of Industrial Science, University of Tokyo, Meguro-ku, Tokyo 153-8505, Japan*
(Received 27 February 2007; revised manuscript received 23 April 2007; published 27 July 2007)

It is a fundamental physical problem how a state is selected in a nonequilibrium steady state where the energy is continuously dissipated. This problem is common to phase transitions in liquids under shear flow and those in solids under deformation or electric current. In particular, soft matter often exhibits a strong nonlinear response to an external field, since its structural susceptibility to the external field is extremely large due to its softness and flexibility. Here we study the nucleation and growth process of the lamellar phase from the sponge phase under shear flow in a bilayer-forming surfactant system. We found an interesting shape selection of lamellar nuclei under shear flow between multilamellar vesicles (onions) and cylinders (leeks). These two types of behavior are separated sharply at a critical shear rate: a slight change of the shear rate is enough to switch one behavior to the other. We also found that, under a sufficiently strong shear flow, nucleated onions decrease their size with time, and eventually transform into leeks. This suggests that leeks may be the stable morphology under steady shear flow. However, the stability is limited only to the lamellar-sponge coexistence region. When a system enters into the lamellar phase region by further cooling, leeks lose their stability and break up into rather monodisperse onions, presumably via Rayleigh-like instability of a fluid tube. On the basis of these results, we draw a dynamic state diagram of smectic membrane organization under shear flow.

DOI: 10.1103/PhysRevE.76.011513 PACS number(s): 83.80.Qr, 61.30.St, 82.70.Uv, 83.60.Rs

## I. INTRODUCTION

Nucleation and growth of an ordered phase from a disordered phase is a key kinetic process of first-order phase transitions. This process has been intensively studied both theoretically and experimentally, due to its fundamental importance. In most cases, however, this problem is studied for a quiescent state. Recently, phase ordering under shear flow has attracted considerable attention from both scientific and applications viewpoints. It is of fundamental importance to reveal the principle of pattern selection in a nonequilibrium state. In terms of applications, we may be able to create novel structures that cannot be formed in an equilibrium state without shear. A related important problem is the relation between structural evolution and rheological behavior. On this problem, there have recently been extensive studies on the behavior of complex fluids such as polymer solutions, surfactant solutions, colloidal suspensions, and emulsions under shear flow [1–6]. These fluids often exhibit a strongly nonlinear response to shear fields, reflecting the soft structural response to shear flow, and sometimes exhibit shear banding (spatially inhomogeneous flow) [7]. Chaotic or nonlinear oscillatory responses to shear fields have also been reported [8,9]. This complex spatiotemporal ordering behavior in a nonequilibrium state is also a matter of current interest.

It is the aim of this paper to shed further light on the problem of pattern selection of soft matter in a nonequilibrium steady state. Here, we study a morphological selection of lamellar domains upon continuous cooling under a steady shear flow in bilayer-forming surfactant and water mixtures [10–18]. One of the most striking phenomena in these systems is the formation of multilamellar vesicles (onions), induced by the application of shear flow to the lamellar phase [10,11,17–24]. For onion formation, both nucleation [18] and a bulk instability scenario [10,19,24] have been suggested. The size of the onions formed from a lamellar ($L_\alpha$) phase is known to obey $R_c \sim \dot{\gamma}^{-1/2}$ in steady state [9–11,23,25], whereas the characteristic length just before onion formation obeys $R_c \sim \dot{\gamma}^{-1/3}$ [19,24]. The size of onions formed from $L_\alpha$-sponge ($L_3$) coexistence is, on the other hand, known to obey $R_c \sim (\sigma/\eta)\dot{\gamma}^{-1}$, where $\sigma$ is the interfacial tension and $\eta$ is the shear viscosity [1,2,17,23,26,27]. Furthermore, Panizza *et al.* reported that a large stepwise increase of shear induces the breakup of onion droplets into smaller ones of an equal size without any elongation [26]. In phase-separating polymer solutions [2,3] and colloidal suspensions [6], on the other hand, it was reported that strings aligning along the flow direction are formed under a high shear rate, and the tube radius $R_t$ is proportional to $\dot{\gamma}^{-1/3}$. In a mixture of sodium bis(2-ethyl-hexyl) surfo-succiate (AOT) and brine, Courbin *et al.* found stringlike elongated structures, which were considered to be made of the sponge phase [9]. Similar multilamellar cylinders (leeks) [25,28,29] and ribbons [30] were also reported for lyotropic liquid crystals under shear.

Here, we experimentally study nucleation of the lamellar phase from the homogeneous sponge phase upon cooling under a steady shear flow. We use a binary mixture of nonionic surfactants and water: Nonionic surfactants spontaneously form bilayer membranes, which further form lamellar or sponge structures, depending upon the temperature and the concentration. In our experiments, we keep the shear rate constant and decrease the temperature at a constant cooling

*Present address: Core Technology Research Center, Ricoh Company, Ltd. 16-1 Shinei-cho, Tsuzuki-ku, Yokohama, 224-0035, Japan.
†Author to whom correspondence should be addressed. tanaka@iis.u-tokyo.ac.jp

 

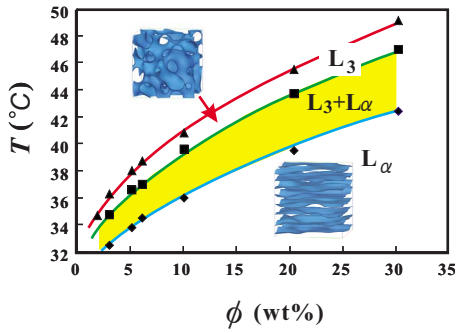


FIG. 1. (Color online) Phase diagram of the $C_{10}E_3$-water mixture. The $L_\alpha$-$L_3$ coexistence region is painted yellow.

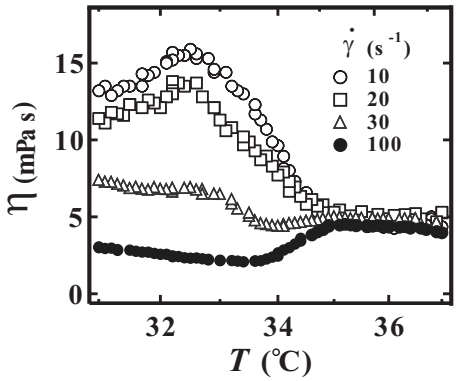


FIG. 2. $T$ dependence of $\eta$ for different shear rates for $\phi$ =5 wt %. The shape of the curves changes between $\dot{\gamma}$=20 and 30 $s^{-1}$. The cooling rate was 0.1 K/min.

rate. Thus, the formation of the lamellar phase is primarily induced by a temperature reduction, but shear flow affects the nucleation and growth process of the lamellar phase significantly. We note that this is different from an often-used experimental procedure, in which the temperature is kept constant and the shear rate is changed. In this case, shear flow is the main driving force of a transition. We describe the details of our experimental results and implications below.

The organization of this paper is as follows. In Sec. II, we describe details of our experiments. In Sec. III, we show the experimental results and discuss them. In Sec. IV, we summarize our paper.

## II. EXPERIMENT

The system we used is a mixture of triethyleneglycol mono-*n*-decyl ether ($C_{10}E_3$) and water. $C_{10}E_3$ is a nonionic surfactant and it spontaneously forms bilayer membranes in a certain region of the temperature $T$ and surfactant concentration $\phi$, when it is dispersed in water (see [20] for the overall phase diagram). The phase diagram is shown in Fig. 1 (see also [20,31]). The membranes further form a higher-order structure, such as a sponge or lamellar structure. At a rather dilute surfactant concentration, the $L_3$ phase transforms into the $L_\alpha$ phase, passing through the coexistence region upon temperature reduction (see Fig. 1), indicating that the $L_3$-$L_\alpha$ transition is a first-order phase transition. The lamellar structure is stabilized by Helfrich repulsions between membranes of purely entropic origin. In the coexistence region, membranes spontaneously form onions (see, e.g., [31,32]). The membrane thickness is about 2.8 nm. For low $\phi$ ($\sim$ a few percent), the intermembrane spacing $d$ can reach the order of a few hundred nanometers, comparable to the wavelength of the visible light. Rheological measurements are performed by a rheometer (Reologica Instruments, StressTech rheometer) in a cone-plate geometry (cone angle 1° and diameter 4 cm). Evaporation of a sample was prevented by saturating the air in the shearing cell with the water vapor. This is achieved by placing a sealing cover over the cell. The samples were presheared for 5 min under $\dot{\gamma}$ =10 $s^{-1}$ in each experiment.

For structural observation under shear, we used a shearing cell (Linkam CSS-450) equipped with an optical microscope (Olympus, BH2) and a high-speed camera (Vision Research, Phantom V5.0). Usage of a high-speed camera is essential to observe morphology without flow-induced image distortion. This shearing cell is made of two parallel glass plates (diameter 3 cm) whose gap was set to 100 $\mu$m. Although the shear field in a parallel plate geometry is not uniform, we confirmed that the local shear rate at an observation point where a morphological transition is observed in this cell coincides well with the shear rate where the corresponding rheological transition is observed by the above rheometer. This coincidence may reflect the quite slow material transport along the radial direction due to the gradient in the shear rate. Furthermore, since we did not notice any dependence of structures on the depth of the focal plane (along the shear gradient direction), we believe that in our experiments the shear rate is uniform in a macroscopic sense in the shearing cell, and only inhomogeneous on the length scale of the structures observed; in other words, there is no macroscopic inhomogeneity. These facts may rationalize the comparison of rheological and optical microscopy measurements in a direct manner.

## III. RESULTS AND DISCUSSION

### A. Rheological signature of two types of nucleation behavior

First we show the $T$ dependence of the viscosity $\eta$ of two systems ($\phi$=5 and 10 wt %) upon cooling through the $L_3$-$L_\alpha$ transition under several shear rates in Figs. 2 and 3, respectively. Upon cooling from the $L_3$ phase to the $L_3$-$L_\alpha$ coexistence region with a rate of 0.1 K/min, the $L_3$-$L_\alpha$ transition occurs. We found the following surprising behavior: for low shear rates, $\eta$ increases when the $L_\alpha$ phase is nucleated, whereas for high shear rates, $\eta$ decreases. A small change of the shear rate leads to an entirely different $T$ dependence of $\eta$: A sharp bifurcation occurs at a critical shear rate $\dot{\gamma}_c$, which is around 30 $s^{-1}$ for 5 wt % [33] and between 750 and 760 $s^{-1}$ for 10 wt %.

Figure 4 shows the dependence of $\dot{\gamma}_c$ on the cooling rate. For a cooling rate faster than 0.1 K/min, $\dot{\gamma}_c$ decreases with an increase in the cooling rate. For a cooling rate below 0.1 K/min, on the other hand, $\dot{\gamma}_c$ becomes more or less independent of the cooling rate. This means that the character-

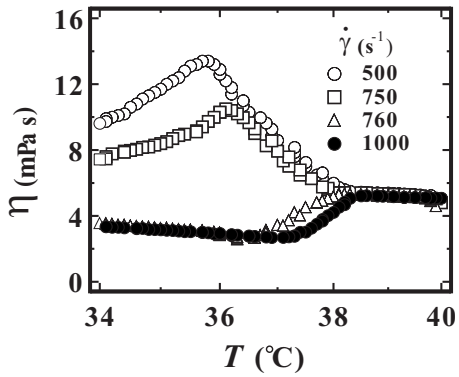


FIG. 3. $T$ dependence of $\eta$ for different shear rates, for $\phi=10$ wt %. The shape of the curves change between $\dot{\gamma}=750$ and 760 $s^{-1}$. The cooling rate was 0.1 K/min.

istic rate of nucleation of the $L_\alpha$ phase is faster than 0.1 K/min. If a cooling rate is too slow, on the other hand, evaporation of a sample starts to cause a problem even under sealing. So we mainly employed the cooling rate of 0.1 K/min. The data shown below were measured with this cooling rate.

Here we show the sharpness of this bifurcation, or how sharply the viscosity behavior upon cooling depends upon the shear rate in Figs. 5 ($\phi=7$ wt %) and 6 ($\phi=10$ wt %). For both cases, we perform sequential experiments by keeping the same sample in the rheometer for different shear rates. After one experiment, we heated the sample to form the homogeneous sponge phase and presheared it to have a reproducible initial shear rate. With this sequential procedure, the critical shear rate can be determined to a very high accuracy (on the order of 1 $s^{-1}$). This surprising sensitivity seems to characterize this bifurcation phenomenon controlled by the shear rate. We note that this level of sensitivity applies only to the above special procedure. For example, both Figs. 3 and 6 are for $\phi=10$ wt %, but there is a small difference in $\dot{\gamma}_c$ between the two measurements, which used different samples of the same composition: In Fig. 6, the bifurcation is observed when the shear rate is changed only from 761 to 763 $s^{-1}$, whereas, in Fig. 3, the transition has already occurred for $\gamma=760$ $s^{-1}$. Note that these two results

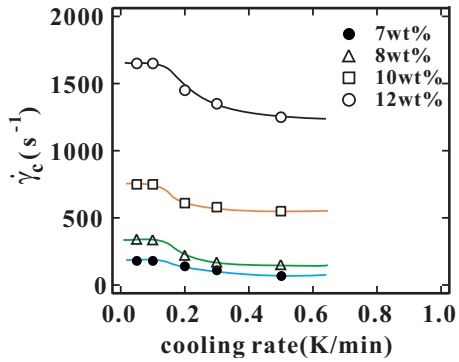


FIG. 4. (Color online) Dependence of the critical shear rate $\dot{\gamma}_c$ on the cooling rate. $\dot{\gamma}_c$ becomes independent of the cooling rate below 0.1 K/min.

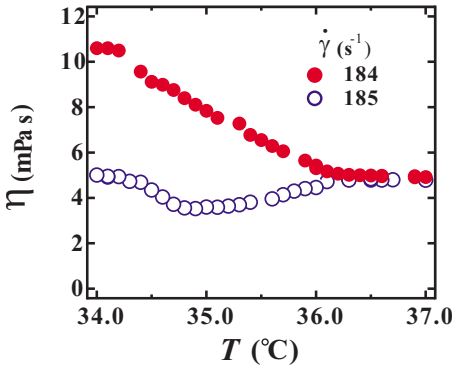


FIG. 5. (Color online) $T$ dependence of $\eta$ for two different shear rates 184 and 185 $s^{-1}$ for $\phi=7$ wt %. Cooling from 37 °C (sponge phase) to 34 °C (lamellar phase) (0.1 K/min). Bifurcation of the viscosity-temperature pattern occurs at a critical shear rate $\dot{\gamma}_c$. For $\dot{\gamma}=184$ $s^{-1}$, the final viscosity is higher than that of the sponge phase, while, for $\dot{\gamma}=185$ $s^{-1}$, it is lower than that of the sponge phase.

are from independent measurements, and not from sequential measurements.

### B. Morphological signature of two types of nucleation behavior

To investigate the cause of the two types of $\eta$-$T$ patterns, we made optical microscope observations. Figure 7 shows optical microscope images of a sample ($\phi=5$ wt %; $\dot{\gamma}_c=30$ $s^{-1}$) during the temperature reduction from 36.5 °C ($L_3$ phase). For $\dot{\gamma}<\dot{\gamma}_c$ [Figs. 7(a)–7(c)], the $L_\alpha$ phase is first nucleated as deformed onions. Upon further cooling, the onions grow in size and the number density of onions also increases, and finally the system is filled up predominantly with polydisperse onions. For $\dot{\gamma}>\dot{\gamma}_c$ [Figs. 7(d)–7(f)], on the other hand, the $L_\alpha$ phase emerges as leeks [34], aligning along the flow direction. Upon further cooling in the $L_3$-$L_\alpha$ coexistence region, the number density of leeks increases,

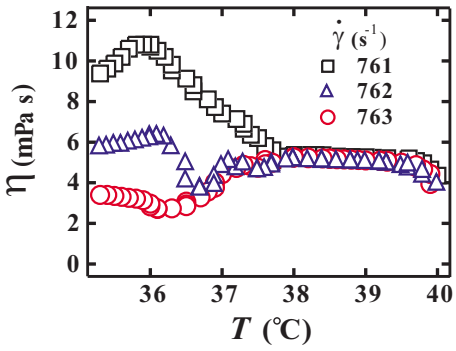


FIG. 6. (Color online) $T$ dependence of $\eta$ for three different shear rates 761, 762, and 763 $s^{-1}$ for $\phi=10$ wt %. Cooling from 40 °C (sponge phase) to 35 °C (lamellar phase) (0.1 K/min). Bifurcation of the viscosity-temperature pattern occurs at a critical shear rate $\dot{\gamma}_c\sim762$ $s^{-1}$. For $\dot{\gamma}=761$ $s^{-1}$, the final viscosity is higher than that of the sponge phase, while, for $\dot{\gamma}=763$ $s^{-1}$, it is lower than that of the sponge phase.

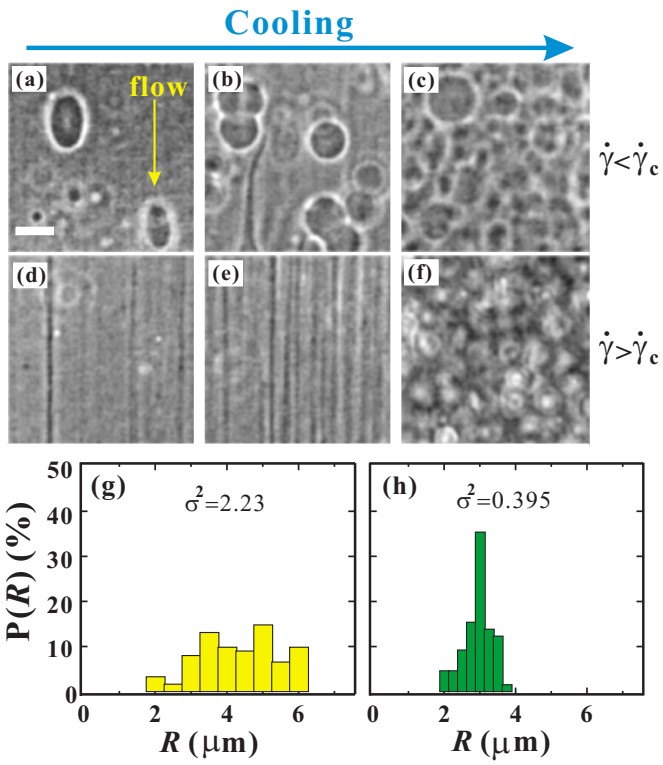


FIG. 7. (Color online) Optical microscopy images under shear flow at $\phi$=5 wt %. Images (a), (b), and (c) are observed at $T$ =34.7, 34.5, and 32.0 °C, respectively, for $\dot{\gamma}$=3.75 $s^{-1}$ < $\dot{\gamma}_c$. Images (d), (e), and (f), are, on the other hand, observed at $T$=34.7, 34.5, and 33.5 °C, respectively, for $\dot{\gamma}$=150 $s^{-1}$ > $\dot{\gamma}_c$. The scale bar corresponds to 20 $\mu$m. (g) and (h) are the probability distributions of the radius $R$ of onions, $P(R)$, for $\dot{\gamma}$=3.75 (c) and 150 $s^{-1}$ (f), respectively. The vertical axis is the percentage of onions of a particular range of $R$ among 60 onions, which are randomly chosen. Onions formed under $\dot{\gamma}$=150 $s^{-1}$ are much more monodisperse than those formed under $\dot{\gamma}$=3.75 $s^{-1}$.

but their thickness remains more or less the same. When the temperature is further lowered into the $L_\alpha$ phase region, where there remains no $L_3$ phase outside leeks, the leek structure is destabilized and breaks up into rather monodisperse onions [see Fig. 7(f)]. Although in Fig. 7 we show only two cases, where $\dot{\gamma}$ is much higher and lower than $\dot{\gamma}_c$, the basic features are common even rather near the critical shear rate.

We also confirmed by microscopy observation that, if we stop shearing after the formation of leeks, the leeks break up into onions within about 10 s. This breakup is due to Rayleigh-like instability of a fluid tube [35]. This indicates that leeks are stable only under shear.

### C. Nucleation of the lamellar phase under shear

Figure 8 demonstrates the $\dot{\gamma}$ dependence of the temperature width of the coexistence region, $\Delta T$. We estimate $\Delta T$ from the distance between the upper inflection point and the peak temperature of the $T$ dependence of $\eta$. $\Delta T$ steeply decreases with an increase in the shear rate $\dot{\gamma}$, accompanying a small jump at $\dot{\gamma}_c$. Above $\dot{\gamma}_c$, the $\dot{\gamma}$ dependence of $\Delta T$ becomes weak. We note that, at $\dot{\gamma}$=0, $\Delta T$ should coincide with the equilibrium value (see Fig. 1). As can be seen in Figs. 2 and 3, the onset of the coexistence region upon cooling, or the stability limit of the $L_3$ phase, is rather insensitive to $\dot{\gamma}$. Thus, the change in $\Delta T$ is primarily due to the onset of the $L_\alpha$ phase region upon cooling. This apparently looks consistent with the fact that, under shear flow, the $L_\alpha$ phase is more favored than the $L_3$ phase, reflecting that the $L_\alpha$ phase presents less resistance to the applied flow. However, since the $L_\alpha$ phase is made of onions and is not of a uniform lamellar structure, this change may reflect the degree of increase of the volume fraction of the lamellar phase (onions or leeks) upon cooling. The rate of increase is faster for a higher shear rate. The discontinuous change of $\Delta T$ at $\dot{\gamma}_c$ seems to indicate that leek structures flow more easily than onion structures. It may be worth mentioning that the onion structure formed below $\dot{\gamma}_c$ is not necessarily a steady-state structure, as will be shown later. To make the mechanism clear, further studies are necessary.

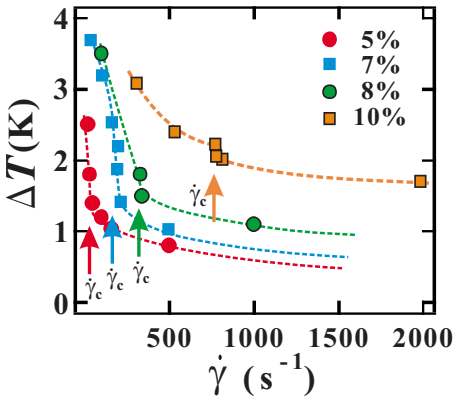


FIG. 8. (Color online) $\dot{\gamma}$ dependence of the temperature width of the coexistence region, $\Delta T$. Its dependence becomes significantly weaker above $\dot{\gamma}_c$.

We confirm that, in the range of $\phi$=5–12 wt %, $\dot{\gamma}_c \cong 7.5\times10^5\phi^3$ $s^{-1}$, as shown in Fig. 9. Although the range of $\phi$ is rather limited, this relation seems to suggest that the switching occurs when $\dot{\gamma}$ exceeds a characteristic time scale, which is proportional to the inverse of a membrane recombination time $\tau \propto \xi^3 \propto \phi^{-3}$, where $\xi$ is the intermembrane spacing. At this moment, the physical process characterized by this shear rate remains elusive, and should be clarified in the future.

Here we characterize the size distribution of onions finally formed in the stable $L_\alpha$ region. Figures 7(g) and 7(h) clearly show that onions formed under $\dot{\gamma}$=150 $s^{-1}$ are much more monodisperse than those formed under $\dot{\gamma}$=3.75 $s^{-1}$. The key origin may be the difference in pattern selection between onions and leeks. Onions are formed primarily by a thermodynamic driving force via the usual nucleation-growth mechanism (a random stochastic process). This growth mechanism may be the origin of polydispersity; e.g., the distribution of the birth times may lead to the size distribution. As will be shown below, onions formed below $\dot{\gamma}_c$ are not in a steady state under shear, and thus the size selection under shear does not necessarily operate in the process. On the other hand, the thickness of leeks may be selected by the

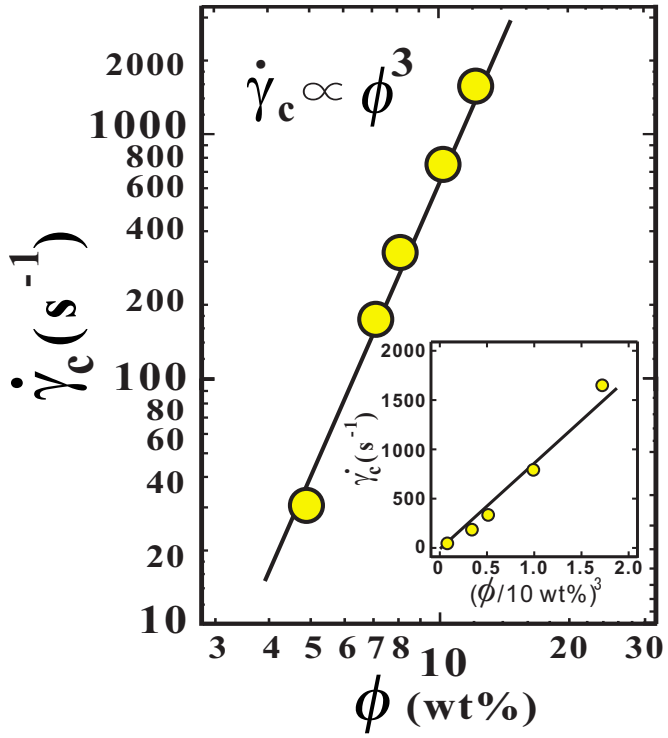


FIG. 9. (Color online) $\phi$ dependence of the critical shear rate $\dot{\gamma}_c$ for the cooling rate of 0.1 K/min. The inset shows the plot of $\dot{\gamma}_c$ against $(\phi/10\ \mathrm{wt}\ \%)^3$. Both plots support the relation $\dot{\gamma}_c \propto \phi^3$ (see solid lines).

shear rate, and thus it is rather uniform; there is little growth of leeks. Furthermore, onions are formed from leeks by a Rayleigh-like instability characteristic of one-dimensional tubes (leeks) of fluid nature. In this instability, the fastest unstable growth mode of interface fluctuations has the wavelength of a tube size, which leads to the breakup into rather monodisperse droplets of the tube size.

### D. Stability of lamellar domains under steady shear and dynamic phase diagram

So far, we have described the difference in the lamellar nucleation pattern between below and above the following $\dot{\gamma}_c$ under continuous cooling. Now we show results on the stability of nucleated lamellar structures under shear flow at a fixed temperature, using both rheological measurements and microscope observations. Figure 10 shows the result of the rheology experiment for $\phi=10$ wt %, for which $\dot{\gamma}_c=780\ \mathrm{s}^{-1}$. In this experiment, first $(0<t<1500\ \mathrm{s})$ we lowered $T$ from 40 °C ($L_3$ phase) to 37.5 °C ($L_3$-$L_\alpha$ coexistence phase) at the rate of 0.1 K/min. Then $(t>1500)$, we kept $T$ at 37.5 °C. For $\dot{\gamma}=1000\ \mathrm{s}^{-1}$ $(>\dot{\gamma}_c)$, the $L_\alpha$ phase is nucleated as leeks, which leads to the decrease of $\eta$ (see above). Then, after stopping cooling, $\eta$ remains roughly constant with time [36]; consistently, we confirmed by microscopic observation that the leek structure also almost does not change for a long time. This indicates that, at this shear rate, the leek structure is more or less a stable morphology. For $\dot{\gamma}=200\ \mathrm{s}^{-1}$ $(<\dot{\gamma}_c)$, on the other hand, we observed the following interesting behavior. For $\dot{\gamma}<\dot{\gamma}_c$, the $L_\alpha$ phase is nucleated as onions, when the system enters into the $L_3$-$L_\alpha$ coexistence region from the $L_3$ phase region (see above). This leads to a viscosity increase: This might be because onions disturb flow fields as colloids in suspensions. After stopping cooling, $\eta$ first increases gradually, but around 8000 s it suddenly drops, and then becomes almost a constant value, slightly lower than $\eta$ of the initial $L_3$ state.

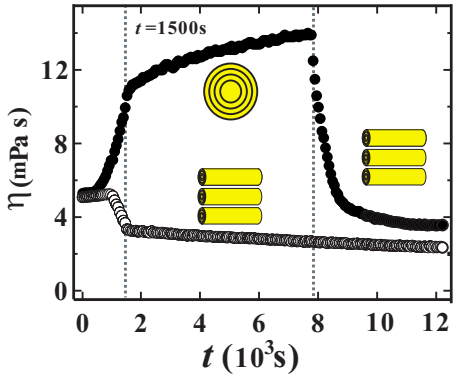


FIG. 10. (Color online) Temporal change of $\eta$ ($\phi=10$ wt %, $\dot{\gamma}_c=780\ \mathrm{s}^{-1}$) for $\dot{\gamma}=1000\ \mathrm{s}^{-1}$ (○) and $200\ \mathrm{s}^{-1}$ (•). For $0<t<1500$ s, we lower the temperature from 40 °C (sponge phase) to 37.5 °C. For $t>1500$ s, we keep the temperature at 37.5 °C under the same shear as that during $0<t<1500$ s. For $\dot{\gamma}=1000\ \mathrm{s}^{-1}>\dot{\gamma}_c$, after the cooling is stopped, the viscosity of the leek phase remains constant. For $\dot{\gamma}=200\ \mathrm{s}^{-1}<\dot{\gamma}_c$, onions are nucleated, and, after the cooling is stopped, the viscosity gradually increases, but at $t=8000$ s the viscosity drastically drops.

To seek the origin of this peculiar viscosity behavior for $\dot{\gamma}<\dot{\gamma}_c$, we observed the process by optical microscopy. Figures 11(a)–11(d) show the structural evolution in a sample of $\phi=10$ wt % when we kept $T$ at 37.5 °C after lowering $T$ from 40 to 37.5 °C at the rate of 0.1 K/min. The shear rate is kept constant at $\dot{\gamma}=200\ \mathrm{s}^{-1}$ $(<\dot{\gamma}_c)$ throughout the experiment. At $t=600$ s, after stopping cooling, the $L_\alpha$ phase is observed as onions, which are nucleated upon cooling. Note that they are thermodynamically preferred to leeks due to the lower interfacial energy per volume. As the time goes on, the size of the onions monotonically decreases, and the polydispersity also decreases (see $t=2000$ and 4000 s), and then onions transform to leeks at $t=8000$ s. The last process corresponds to the sudden drop of the viscosity observed by rheological measurements (Fig. 10). This tells us that leeks are preferred to onions under strong enough shear flow: Unlike onions, leeks do not disturb flow fields, since they align along the flow direction, and furthermore the elastic energy cost of the leek configuration is lower than that of the onion configuration.

When the size of the onions decreases gradually and the polydispersity decreases, $\eta$ gradually increases. The temporal change in the mean size of onions is shown in Fig. 11(e). Here, the point (○) at $t=8000$ s shows the average size of leeks. Although the size of onions continuously decreases, the topology changes discontinuously from spheres to cylinders (no size discontinuity within the resolution), which leads to the sudden drop of $\eta$. An example of the $\dot{\gamma}$ depen-

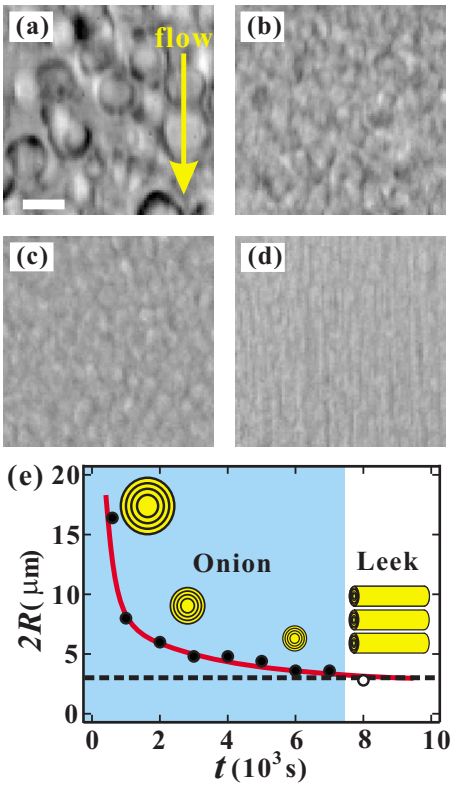


FIG. 11. (Color online) Structural evolution of the $L_\alpha$ phase ($\phi$=10 wt %) observed by optical microscopy in the $L_3$-$L_\alpha$ coexistence region under $\dot{\gamma}$=200 $s^{-1} < \dot{\gamma}_c$. (a)–(d) correspond, respectively, to 600, 2000, 4000, and 8000 s after keeping $T$ at 37.5 °C. After the cooling is stopped, the size of onions gradually decreases with time [see (b) and (c)]. At $t$=8000 s, onions are drastically transformed into leeks [see (d)]. The scale bar corresponds to 20 $\mu$m. (e) shows the temporal change of $2R$. The horizontal dashed line represents the diameter of leeks finally formed, $R_t$.

dence of $R_i$ is shown in Fig. 12. Here, $R_i$ is the initial average radius of onions just after stopping cooling. The size of onions initially increases with time during temperature cooling, but it starts to decrease under shear after stopping cooling. Thus, $R_i$ can be regarded as the maximum average onion radius. In this case, the initial radius of the onions, $R_i$, seems to obey $R_i \propto \dot{\gamma}^{-0.7}$. At this moment, we do not know the underlying mechanism determining $R_i$, and thus the above fitting has no reliable ground. The tube radius $R_t$ is, on the other hand, proportional to $\dot{\gamma}^{-0.5\pm0.2}$. However, we note that this relation for leeks suffer from considerable errors. Thus, it might even be compatible with the corresponding relation for strings formed in phase separation under shear [3,6]: $R_t \propto \dot{\gamma}^{-1/3}$. Scattering experiments, which can pick up the characteristic size more accurately, are highly desirable. Concerning the former relation for onions, we should note that this initial state just after stopping cooling is not in a steady state: $R_i$ may be determined by kinetic factors, such as the growth rate and decay rate of the onion size, and not by a force balance condition, which is valid only for a steady state. Thus, the $R$-$\dot{\gamma}$ relation mentioned above is nothing to do with those described in the Introduction. In other words, the only steady state configuration seems to be the leek structure in these conditions.

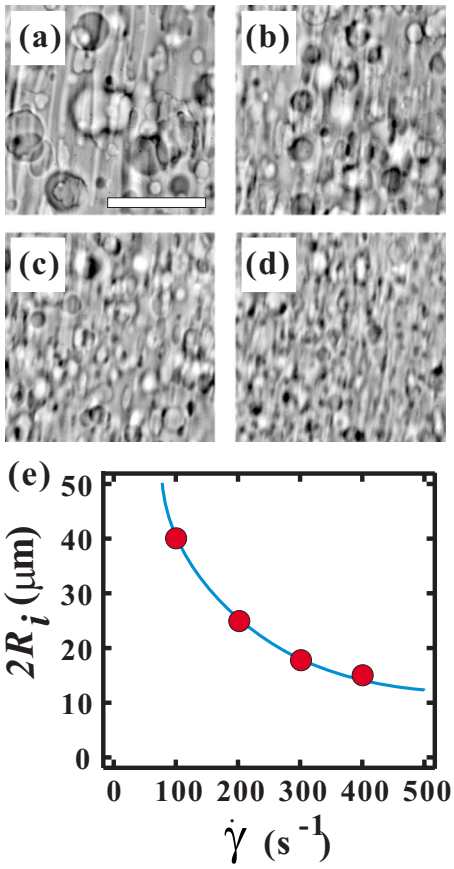


FIG. 12. (Color online) $\dot{\gamma}$ dependence of the initial size of onions, $R_i$, for $\phi$=10 wt %. $\dot{\gamma}$=(a) 100, (b) 200, (c) 300, and (d) 400 $s^{-1}$. Scale bar corresponds to 100 $\mu$m. (e) $\dot{\gamma}$ dependence of $2R_i$, measured from images like (a)–(d). We averaged the diameter of onions for 20 onions randomly chosen, and plotted it in this figure. The solid line is $2R(\dot{\gamma})=1052/\dot{\gamma}^{0.7}$ $\mu$m. Although we do not make any quantitative analysis, we can see that the polydispersity of onions decreases with an increase in $\dot{\gamma}$.

Figure 13 shows the shear-rate dependence of the incubation time for the onion-leek transition. The incubation time fluctuates from measurement to measurement even for the same conditions by $\pm(2-3)\times10^3$ s, but such fluctuations do

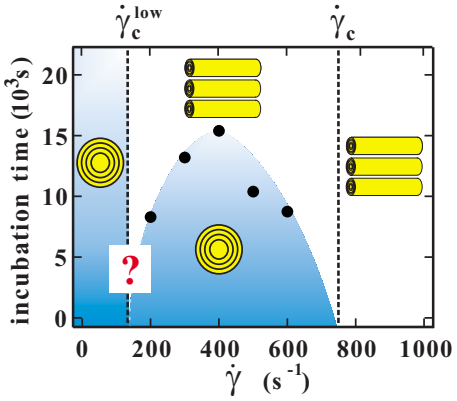


FIG. 13. (Color online) Dynamic state diagram under shear flow for $\phi$=10 wt % and $T$=37.5 °C.

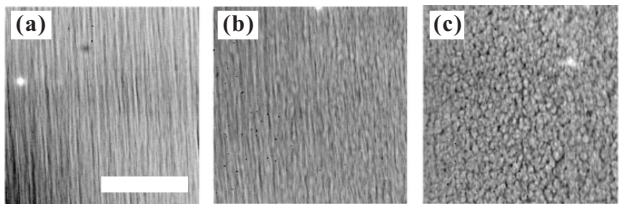


FIG. 14. Microscopy images for $\phi=10$ wt % at about 9000 s after keeping the temperature at $T=37.5$ °C for $\dot{\gamma}=170$ (a), 200 (b), and 230 $s^{-1}$ (c). Scale bar corresponds to 100 $\mu$m.

not alter the overall trend. The distribution of the incubation time may shed further light on the nature of the transition, but this problem remains for future investigation. We experimentally confirmed that onions do not transform to leeks at 50 and 100 $s^{-1}$, at least before $20\times10^3$ s. Although we are not sure whether the incubation time becomes minimum or zero at $\dot{\gamma}_c^{low}$, it may be reasonable to define $\dot{\gamma}_c^{low}$ as a characteristic shear rate. At this moment, we believe that the former may be the case. We locate $\dot{\gamma}_c^{low}$ between 100 and 200 $s^{-1}$ (more precisely, we set the upper bound to 170 $s^{-1}$ instead of 200 $s^{-1}$; see below). Although we cannot completely rule out the possibility that onions transform into leeks after a longer time under shear, we believe that the existence of $\dot{\gamma}_c^{low}$itself may be reasonable, noting that for a quiescent state ($\dot{\gamma}=0$) onions are formed as the stable form [31,32] and there is no transformation to leeks. So we suppose that, below $\dot{\gamma}_c^{low}$, the stable state of the $L_\alpha$ phase is onions, which are formed via nucleation upon cooling. Above $\dot{\gamma}_c$, on the other hand, the $L_\alpha$ phase is nucleated as leeks, which are stable. Between $\dot{\gamma}_c^{low}$ and $\dot{\gamma}_c$, the transformation from onions to leeks takes place after an incubation time. The incubation time exhibits a peak at a certain $\dot{\gamma}$. We confirmed that for a lower shear rate the difference between $R_i$ and $R_t$ is larger, whereas the shrinking rate of the onion radius is faster for larger onions [see, e.g., Fig. 11(e)]. Based on these facts, we speculate that the competition between the amount of the overall size change ($R_i-R_t$) and the rate of the change $dR/dt$ may be the origin of the peak: $\int_{R_i}^{R_t} dR(R_i-R_t)/(dR/dt)$ has a peak at a particular $\dot{\gamma}$. This point needs further careful study.

Figure 14 shows images observed with optical microscopy at about 9000 s after keeping the temperature at $T=37.5$ °C under $\dot{\gamma}=170$ (a), 200 (b), and 230 $s^{-1}$ (c). These images are observed at about the same time in the same sample. There is a spatial change in the shear rate along the radial direction in the shearing cell made of two parallel glass plates. This gradient exists even inside the observation area (i.e., the optical window), which allows us to see the shear-rate dependence of the incubation time in this way. For $\dot{\gamma}=170$ $s^{-1}$, onions already transform into leeks, whereas for $\dot{\gamma}=230$ $s^{-1}$ they remains as onions, which is consistent with the dynamic state diagram shown in Fig. 13.

Next we show the behavior of onions under shear after cooling to a temperature in the $L_\alpha$ phase region. The results are summarized in Fig. 15. In the $L_\alpha$ phase region, onions seem to be stable even for long-time shearing. We also see in Fig. 7(f) that the leek structure is destabilized when a system enters into the $L_\alpha$ phase region: leeks break up into rather

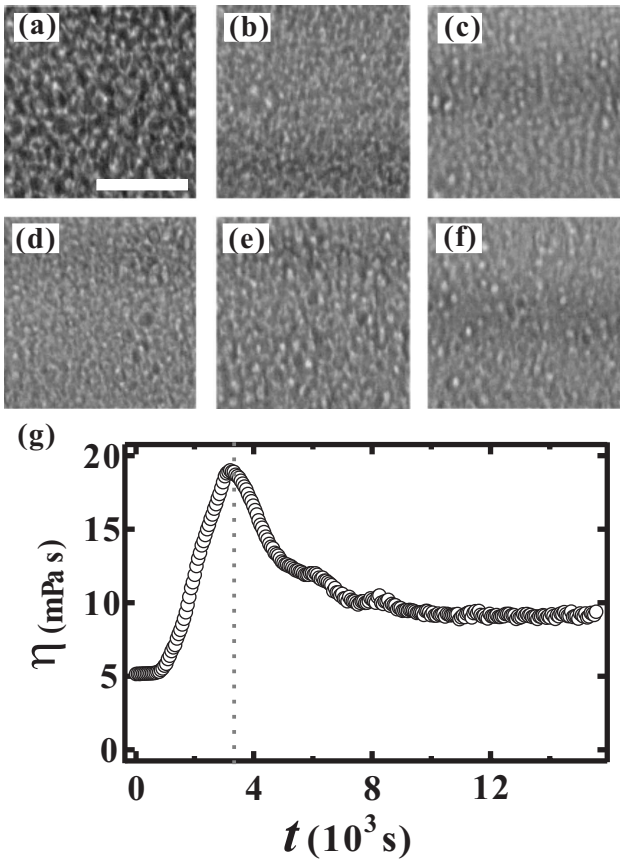


FIG. 15. Images observed with optical microscopy for $\phi=10$ wt % at (a) 1000, (b) 2000, (c) 6000, (d) 7000, (d) 10 000, and (f) 14 000 s after keeping the temperature at $T=35$ °C for $\dot{\gamma}=200$ $s^{-1}$. Scale bar corresponds to 100 $\mu$m. (g) Viscosity change during cooling from 40.0 to 35 °C ($t<3000$ s) and keeping the temperature at this value. The viscosity reaches a stationary state after 8000 s.

monodisperse onions there. These results indicate that the existence of the $L_3$ phase is indispensable for the stability of the leek structure. This viscosity asymmetry between the inside and outside of a string may be a general requirement for stabilization of string structures, including other cases [3,6].

### E. Summary of our observation

For a quiescent state and a weak shear flow ($\dot{\gamma}<\dot{\gamma}_c^{low}$), onions are nucleated and survive for a very long time. In this case, onions seem to be more favored than leeks. Note that the former have less interfacial energy than the latter, although the elastic energy cost is larger in the former than in the latter. For an intermediate shear rate ($\dot{\gamma}_c^{low}<\dot{\gamma}<\dot{\gamma}_c$), leeks are more favored than onions, but a cooling process leads to a metastable onion state, and the transformation between onions and leeks may present a barrier to overcome. It seems that this barrier is reduced with a decrease in the onion size, and becomes of the order of the thermal energy when the onion size reaches the tube size of leeks to be formed at that shear rate. Onions gradually reduce their size. Then when they become a critical size $R_t$, they transform into leeks (see

Fig. 11). We believe that the existence of $\dot{\gamma}_c^{low}$ itself is robust since, at least for a quiescent state, leeks cannot exist as a stable morphology. At this moment, we do not understand what physical factors determine the initial size of onions, $R_i$, just after stopping cooling. The formation of large-size metastable onions may reflect that the rate of increase in the onion radius $R$ is probably much faster than the rate of decrease in $R$ during the cooling process. In other words, onion growth driven by a thermodynamic driving force is faster than shear-induced decrease in the onion size. For a high shear rate ($\dot{\gamma} > \dot{\gamma}_c$), leeks are immediately formed, without passing through onions as an intermediate structure. At least on the level of optical microscopic observation, we did not see any indication of such an intermediate structure before the formation of leeks. The process and mechanism of leek formation remain for future investigation.

### F. Comparison with related studies

Finally, it is worth noting that similar stringlike structures are reported for (a) $C_{10}E_3/D_2O$ by Richtering and coworkers [25,28,29] and (b) a mixture of brine, surfactant, and cosurfactant by Cristobal *et al.* [30]. For case (a), the system is identical to the one we used, but $\phi$ was 40 wt % and $\dot{\gamma} = 10\ s^{-1}$. According to our relation $\dot{\gamma}_c \cong 7.5 \times 10^5 \phi^3\ s^{-1}$ (see Fig. 4), $\dot{\gamma}_c$ estimated for their concentration is beyond $10^4\ s^{-1}$. They observed a leek structure as an intermediate structure upon the transformation of planar lamellae to onions in the lamellar phase region. This is markedly different from our observation that leeks exist only in the $L_\alpha$-$L_3$ coexistence region. The structure observed in their experiments was interpreted as either a multilamellar cylinder or a coherent stripe buckling with the wave vector of the undulation in a neutral (or vorticity) direction [25]. Thus, their observation seems to have no direct connection to ours. For case (b), it was proposed that the structure is not a cylinder, but a ribbon. The ribbons are observed as a steady state in the $L_\alpha$-$L_3$ coexistence region, which is similar to our observation. However, the ribbons are destabilized and fragmented into rather monodisperse onions for a high shear rate, which is very different from our observation. The similarity and the difference suggest very rich dynamic behavior under shear, and drawing an overall picture covering these phenomena is an interesting problem, remaining for future investigation. Finally, we stress that our experimental procedure (temperature scanning) is different from those of the other cases mentioned here, as explained in the Introduction.

## IV. CONCLUSION

In sum, we demonstrated an interesting shape selection upon nucleation of lamellar domains under shear flow, and the stability of the nucleated domains. For a low shear rate, the lamellar phase is nucleated as onions upon cooling, whereas for a high shear rate the lamellar phase emerges as leeks. These two types of behavior are separated surprisingly sharply at a critical shear rate: less than 1% change of the shear rate is enough to switch one behavior to the other. We also found that, under a sufficiently strong shear flow, nucleated onions decrease their size with time, and eventually transform into leeks. On the basis of these results, we draw a dynamic state diagram of smectic membrane organization under shear flow, which adds an interesting case to the rich spatiotemporal ordering behavior in a nonequilibrium state. This suggests that leeks may be a stable morphology under steady shear flow. However, the stability is limited to only the lamellar-sponge coexistence region. When a system enters into the lamellar phase region by further cooling, leeks lose their stability and break up into rather monodisperse onions, presumably via Rayleigh-like instability of a fluid tube. This provides us not only with a dynamic state diagram of membrane organization under shear flow, but also with a route to the formation of monodisperse onions using shear flow (see also, e.g., [26]). There remain many open questions concerning the physical mechanism of this pattern selection under shear flow, and thus further detailed studies are highly desirable.

## ACKNOWLEDGMENT

This work was partly supported by a Grand-in-Aid for Scientific Research from the Ministry of Education, Culture, Sports, Science and Technology, Japan.

[1] R. G. Larson, *The Structure and Rheology of Complex Fluids* (Oxford University Press, Oxford, 1999).
[2] See, for review, e.g., A. Onuki, J. Phys.: Condens. Matter **9**, 6119 (1997).
[3] T. Hashimoto, K. Matsuzaka, E. Moses, and A. Onuki, Phys. Rev. Lett. **74**, 126 (1995).
[4] K. B. Migler, Phys. Rev. Lett. **86**, 1023 (2001).
[5] P. D. Olmsted, Europhys. Lett. **48**, 339 (1999).
[6] D. Derks, Ph.D. thesis, Utrecht University, 2005.
[7] T. C. B. McLeish and R. C. Ball, J. Polym. Sci., Part B: Polym. Phys. **24**, 1735 (1986); S. Hess and Z. Naturforsch, **30A**, 728 (1975); P. D. Olmsted and P. M. Goldbart, Phys. Rev. A, **41**, 4578 (1990); J.-F. Berret, D. C. Roux, and G. Porte, J. Phys. II **4**, 1261 (1994); R. Makhloufi, J. P. Decruppe, A. Ait-Ali, and R. Cressely, Europhys. Lett. **32**, 253 (1995); P. T. Callaghan, M. E. Cates, C. J. Rofe, and J. B. A. F. Smeulders, J. Phys. II **6**, 375 (1996); P. Espanol, X. F. Yuan, and M. E. Cates, J. Non-Newtonian Fluid Mech. **65**, 93 (1996); N. A. Spenley, X. F. Yuan, and M. E. Cates, J. Phys. II **6**, 551 (1996); P. Boltenhagen, Y. T. Hu, E. F. Matthys, and D. J. Pine, Phys. Rev. Lett. **79**, 2359 (1997); G. Porte, J. F. Berret, and J. L. Harden, J. Phys. II **7**, 459 (1997); C. Grand, J. Arrault, and M. E. Cates, *ibid.*, **7**, 1071 (1997); F. Greco and R. C. Ball, J. Non-Newtonian Fluid Mech., **69**, 195 (1997); P. D. Olmsted and C.-Y. D. Lu, Phys. Rev. E **56**, R55 (1997); J. F. Berret, D. C. Roux, and G. Porte, J. Phys. II **4**, 1261 (1998); D. Bonn, J.

Meunier, O. Greffier, A. Al-Kahwaji, and H. Kellay, Phys. Rev. E **58**, 2115 (1998); H. Tanaka, J. Phys. Soc. Jpn. **69**, 299 (2000); J. B. Salmon, S. Manneville, and A. Colin, Phys. Rev. E **68**, 051503 (2003).

[8] Y. T. Hu, P. Boltenhagen, and D. J. Pine, J. Rheol., **42**, 1185 (1998); C. Meyer, S. Asnacios, C. Bourgaux, and M. Kleman, Mol. Cryst. Liq. Cryst. Sci. Technol., Sect. A **A332**, 531 (1999); R. Bandyopadhyay and A. K. Sood, Europhys. Lett. **56**, 447 (2001); R. Bandyopadhyay, G. Basappa, and A. K. Sood, Phys. Rev. Lett. **84**, 2022 (2000); A.-S. Wunenburger, A. Colin, J. Leng, A. Arnéodo, and D. Roux, *ibid.* **86**, 1374 (2001); J.-B. Salmon, A. Colin, and D. Roux, Phys. Rev. E **66**, 031505 (2002); W. M. Holmes, M. R. Lopez-Gonzales, and P. T. Callaghan, Europhys. Lett. **64**, 274 (2003); P. Panizza, L. Courbin, G. Cristobal, J. Rouch, and T. Narayanan, Physica A **332**, 38 (2003); D. Lootens, H. Van Damme, and P. Hébraud, Phys. Rev. Lett. **90**, 178301 (2003); M. Das, B. Chakrabarti, C. Dasgupta, S. Ramaswamy, and A. K. Sood, Phys. Rev. E **71**, 021707 (2005); R. Ganapathy and A. K. Sood, Phys. Rev. Lett. **96**, 108301 (2006).

[9] L. Courbin, A. Benayad, and P. Panizza, Phys. Rev. E **73**, 011501 (2006).

[10] O. Diat, F. Nallet, and D. Roux, J. Phys. II **3**, 1427 (1993).

[11] J. Bergenholtz and N. J. Wagner, Langmuir **12**, 3122 (1996).

[12] J. Yamamoto and H. Tanaka, Phys. Rev. Lett. **77**, 4390 (1996).

[13] H. Tanaka, M. Isobe, and H. Miyazawa, Phys. Rev. E **73**, 021503 (2006).

[14] J. Berghausen, J. Ziphel, P. Lindner, and W. Richtering, Europhys. Lett. **43**, 683 (1998).

[15] S. W. Marlow and P. D. Olmsted, Eur. Phys. J. E **8**, 485 (2002).

[16] R. Bruinsma and Y. Rabin, Phys. Rev. A **45**, 994 (1992).

[17] A. S. Wunenburger, A. Colin, J. Leng, A. Arnéodo, and D. Roux, Phys. Rev. Lett. **86**, 1374 (2001).

[18] A. Léon, D. Bonn, J. Meunier, A. Al-Kahwaji, and H. Kellay, Phys. Rev. Lett. **86**, 938 (2001).

[19] A. Zilman and R. Granek, Eur. Phys. J. B **11**, 593 (1999).

[20] T. D. Le, U. Olsson, K. Ortensen, J. Ziphel, and W. Richtering, Langmuir **17**, 999 (2001).

[21] L. Ramos, D. Roux, P. D. Olmsted, and M. E. Cates, Europhys. Lett. **66**, 888 (2004).

[22] L. Courbin, R. Pons, J. Rouch, and P. Panizza, Europhys. Lett. **61**, 275 (2003).

[23] P. Panizza, A. Colin, C. Coulon, and D. Roux, Eur. Phys. J. B **4**, 65 (1998).

[24] L. Courbin, J. P. Delville, J. Rouch, and P. Panizza, Phys. Rev. Lett. **89**, 148305 (2002).

[25] F. Nettesheim, J. Zipfel, U. Olsson, F. Renth, P. Linder, and W. Richtering, Langmuir **19**, 3603 (2003).

[26] L. Courbin, W. Engl, and P. Panizza, Phys. Rev. E **69**, 061508 (2004); L. Courbin, P. Panizza, and J. B. Salmon, Phys. Rev. Lett. **92**, 018305 (2004).

[27] L. Courbin, G. Cristobal, J. Rouch, and P. Panizza, Europhys. Lett. **55**, 880 (2001).

[28] J. Zipfel, F. Nettesheim, P. Linder, T. D. Le, U. Olsson, and W. Richtering, Europhys. Lett. **53**, 335 (2001).

[29] F. Nettesheim, U. Olsson, P. Linder, and W. Richtering, J. Phys. Chem. B **108**, 6328 (2004).

[30] G. Cristobal, J. Rouch, P. Panizza, and T. Narayanan, Phys. Rev. E **64**, 011505 (2001).

[31] Y. Iwashita and H. Tanaka, Nat. Mater. **5**, 147 (2006).

[32] Y. Iwashita and H. Tanaka, Phys. Rev. Lett. **98**, 145703 (2007).

[33] This estimation of $\dot{\gamma}_c$ relies on the fact that the shape of the $T$ dependence of $\eta$ at $\dot{\gamma}_c=30\ \mathrm{s}^{-1}$ for $\phi=5$ wt % (see Fig. 2) is characteristic of that just around the critical shear rate $\dot{\gamma}_c$ (see the curve for $\dot{\gamma}=762\ \mathrm{s}^{-1}$ in Fig. 6). We always saw this particular shape of the $T$ dependence of $\eta$ just around $\dot{\gamma}_c$.

[34] Our observation alone does not tell us whether the stringlike structures are cylindrical leeks or ribbons [30] (e.g., leeks with an ellipsoidal cross section), but here we use the term "leeks" to represent them. A reason is that the Rayleigh-like instability is indicative of a cylindrical geometry. We need to perform scattering and birefringence experiments to unambiguously determine the internal membrane structure in this apparently stringlike object.

[35] This Rayleigh-like instability is also known as the "pearling instability" of cylindrical membranes [R. Bar-Ziv, T. Tlusty, and E. Moses, Phys. Rev. Lett. **79**, 1158 (1997)].

[36] The origin of the gradual decrease of $\eta$ with time is not clear at this moment. There might be a gradual change in the radius of leeks, although our resolution in morphological observations is not high enough to detect such a change even if it exists.